Meteoritics & Planetary Science 40, Nr 7, 981–987 (2005)
Abstract available online at http://meteoritics.org

MALDI analysis of presolar nanodiamonds: Mass spectrometric determination of the mass distribution of nanodiamonds from meteorites and a technique to manipulate individual nanodiamonds

Ian C. LYON

School of Earth, Atmospheric and Environmental Sciences, The University of Manchester, M13 9PL, UK
E-mail: Ian.Lyon@manchester.ac.uk

(Received 24 March 2005; revision accepted 29 June 2005)

Abstract–This paper describes the use of matrix-assisted laser desorption and ionization (MALDI) to measure the mass distribution of nanodiamonds extracted from meteorites. The techniques used to prepare and mass analyze nanodiamond samples from the Murchison (CM2) and Allende (CV3) meteorites are described. The mass spectra of nanodiamonds (peaking at between 1×10^4–1.5×10^4 Daltons) are compared with size distributions obtained by point-counting transmission electron microscopy (TEM) images obtained elsewhere and reasonable agreement is found. The implications of the ability to produce and mass analyze a beam of nanodiamonds are explored.

INTRODUCTION

Presolar nanodiamonds are diamonds with a mean size of ~2 nm that are extracted from meteorites. They have many characteristics that suggest that they were formed in a supernova environment and seeded into the presolar nebula. They were first identified by Lewis et al. (1987) following the purification and identification of the carrier of an unusual xenon component, Xe-HL (enriched in the heavy xenon isotopes ^{136,134}Xe and light isotopes ^{124,126}Xe relative to ^{128,130,132}Xe) (Reynolds and Turner 1964; Clayton 1989; Howard et al. 1992; Anders and Zinner 1993; Huss and Lewis 1994). The acid resistant residue that carried Xe-HL was known for many years as Cδ (Lewis et al. 1987), but since the identification of Cδ as nanometer-scale diamonds, they are normally now referred to as nanodiamonds.

The carbon isotope composition of nanodiamonds is close to that of terrestrial carbon isotope ratios ($\delta^{13}C = -32‰$ to $-38‰$ PDB (Lewis et al. 1987; Russell et al. 1991, 1996), but some of the elements trapped by the nanodiamonds show deviations from solar system isotope abundances. The most abundant minor constituent is nitrogen with $\delta^{15}N = -348 \pm 7‰$, (Lewis et al. 1987; Russell et al. 1996). However, although this deviates considerably from the terrestrial nitrogen isotope ratio, a recent measurement of $\delta^{15}N \sim -350‰$ in the Jovian atmosphere by the Galileo spacecraft (Owen et al. 2001) may mean that a value of $\delta^{15}N \sim -350‰$ relative to terrestrial nitrogen represents solar system average and the terrestrial value is anomalously enriched in ^{15}N. If that were the case, then nanodiamonds would contain solar system isotopically normal nitrogen.

The evidence for a presolar origin of nanodiamonds rests largely on the fact that they are the carrier of Xe-HL, although only approximately 1 in 10^6 nanodiamonds carry a xenon atom (Russell et al. 1991). Deviations from solar system isotope abundances for other elements trapped in nanodiamonds have been found (Lewis et al. 1991; excesses in ^{128,130}Te: Richter et al. 1998; small excesses in ^{128,130}Te and ^{110}Pd: Maas et al. 2001; no deviations from terrestrial isotope abundances in Pt: Merchel et al. 2003).

An unexplained question on the properties of Xe-HL is that the enrichments of the light and heavy isotopes of xenon appear strongly coupled, so that to good approximation, Xe-HL appears to be a single component (Huss and Lewis 1994). This is puzzling, since Xe-L (enrichment in the p-process light xenon isotopes ^{124,126}Xe) and Xe-H (enrichment in the r-process heavy isotopes ^{134,136}Xe) are thought to be produced in separate regions of supernovae (Clayton 1989; Clayton et al. 1995) and the process(es) that would be required to mix the components together to make Xe-HL a robust, inseparable mixture of Xe-L and Xe-H are as yet unclear.

Progress in understanding the abundance of r-process isotopes in nanodiamonds has been achieved by Ott's model (1996), in which it is proposed that the probability of trapping and implantation of elements is related to their pre-cursor half lives, a model which the isotope data seem to support (Qian et al. 1999). For Xe-HL, it is possible that there are separate nanodiamond carriers of Xe-L and Xe-H and that these were

intimately mixed either in interstellar space or in the presolar nebula, although Fisenko et al. (2004) presented evidence that Xe-HL existed as a single xenon component prior to its trapping in nanodiamonds.

The question therefore arises as to whether the approximately solar system normal isotope values of carbon and nitrogen in nanodiamonds are due to summing an isotopically diverse population, all of which are presolar (but the average is coincidentally close to solar system normal), or whether C and N isotope ratios of almost all nanodiamonds are individually close to solar system average C and N ratios and only a small fraction are presolar, carrying anomalous Xe, Te, and Pd (and possibly with anomalous C and N ratios). The absence of nanodiamonds in interplanetary dust particles argues that the vast majority may have been formed within the solar system (Dai et al. 2002).

The only way to address this question would be through the analysis of individual nanodiamonds, but carbon isotope analyses typically require 10^{11} nanodiamonds and minor elemental components require correspondingly larger sample sizes, so only bulk averages are ever measured. This has led to efforts to separate nanodiamonds by size to see whether different populations can be distinguished based on their different physical characteristics; some progress in this direction has been achieved (Verchovsky 1998). However, if the carbon isotopic composition of individual nanodiamonds (and, if possible, the more abundant elemental components trapped within nanodiamonds) are ever to be measured, then clearly some method needs to be found to separate and manipulate individual nanodiamonds. This scientific driver formed the primary motivation for the present work.

Separating Individual Nanodiamonds

Measuring the carbon isotopic composition of individual nanodiamonds will be technically very challenging. On average, there are approximately 1000 carbon atoms per nanodiamond, which means that as the bulk nanodiamond $^{13}C/^{12}C$ isotope ratio is close to a solar system mean value of 1/89, then there will only be on average about 11 ^{13}C atoms to 990 ^{12}C atoms per nanodiamond. With such small numbers of atoms per nanodiamond, the $^{13}C/^{12}C$ ratios of individual diamonds will show a wide scatter due to sampling statistics. The question then boils down to whether the standard deviation of $^{13}C/^{12}C$ ratios of individual nanodiamonds is much greater than or equal to the standard deviation of the ratios expected by sampling statistics and whether there are populations of diamonds with distinctly different $^{13}C/^{12}C$ ratios. This question cannot be addressed by this paper, but an essential requirement to be able to tackle this question is the ability to separate and manipulate nanodiamonds individually, which is what is demonstrated here. Given nanodiamond ions that may be separated, accelerated, and manipulated by electric and magnetic fields, it may be possible to mass resolve individual nanodiamonds from contaminating matrix and deliver the nanodiamond ion to a point where it could be completely disrupted, for example, by a powerful laser pulse into its constituent atoms, each being ionized and so measure the isotopic abundances of atoms from individual nanodiamonds.

Such a possibility remains for the future. It is the aim of this paper to demonstrate a technique for separating and manipulating nanodiamonds as individual entities and measuring their mass distribution.

ANALYTICAL METHODS: MALDI ANALYSIS

Matrix-assisted laser desorption and ionization (MALDI) is a well-established technique for obtaining mass spectra of large organic molecules, usually in the fields of biosciences and polymer chemistry (e.g., Nielen 1999; Macha and Limbach 2002; Stump et al. 2002; Murgasova and Hercules 2003). Its present popularity relies on its ability to ionize and accelerate large molecules without damage or fragmentation. The analyte is dissolved and dispersed in an organic matrix (such as sinapinic acid, molecular weight ~200) at a level of about 1 part in 10^4. The analyte is dispersed and locked within the matrix as it crystallizes. At such low concentrations, the individual analyte molecules are separated from each other within the matrix.

The crystallized sample is held at high positive potential as the ion source of a time-of-flight mass spectrometer. When irradiated by an ultraviolet laser (typically an N_2 laser, 337 nm), the matrix absorbs the UV laser light, dissociates and expands out into the vacuum. The analyte molecules are swept up with the expanding cloud of atoms and small molecules from the matrix and some analyte molecules become ionized. This acceleration and ionization mechanism is relatively gentle and results in little or no fragmentation of the large analyte molecules, even though they may have molecular masses of up to 5×10^5 Daltons (Stump et al. 2002; Jurinke et al. 2004). The ions are then all accelerated through the same large potential difference to gain the same kinetic energy and can therefore be mass resolved by the time-of-flight mass spectrometer before detection by an ion detector. A reflectron is often used to improve mass resolution.

Although MALDI is usually used to analyze large organic and biological molecules ranging up to 5×10^5 Daltons, it was realized here that if the nanodiamonds could be considered in a sense as large molecules (typically ~10^4 Daltons), then MALDI analysis may be applicable to their mass analysis and suitable as a means of producing a beam of nanodiamond ions for the manipulation of individual nanodiamonds.

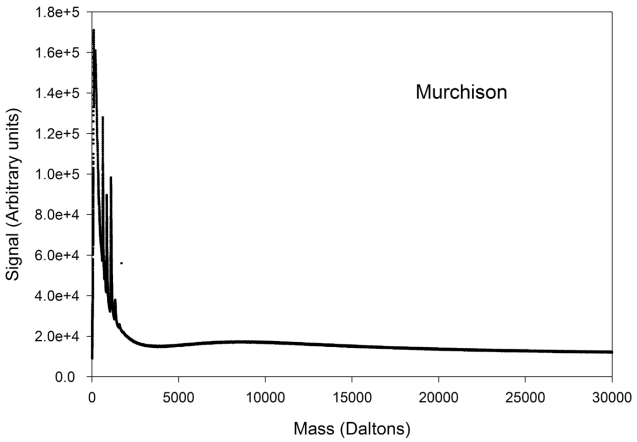

Fig. 1a. A mass spectrum obtained from the Murchison nanodiamond sample mixed with DHB matrix and silver trifluoroacetate. The intensity scale is in arbitrary detector units with a constant zero offset.

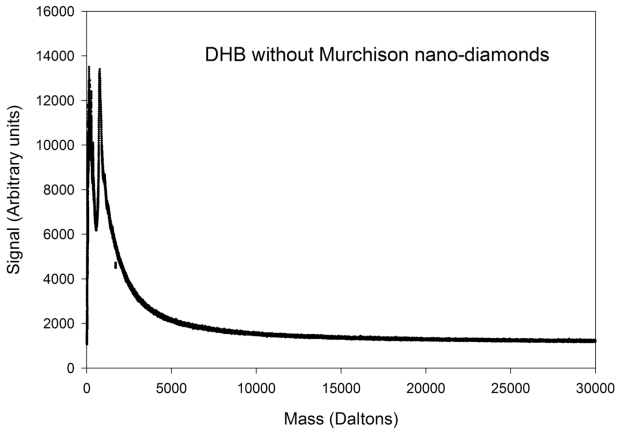

Fig. 1b. A mass spectrum obtained from DHB matrix and silver trifluoroacetate alone.

ANALYTICAL METHODS: SAMPLE PREPARATION AND DATA ACQUISITION

Samples of nanodiamonds prepared by J. Arden were available extracted from the Murchison and Allende meteorites using the acid treatment techniques of Lewis et al. (1987) and Amari et al. (1994). A small quantity was taken up into 4 μL of ultrapure water by ultrasonic agitation. It was impossible to quantify the exact weight of nanodiamond residue removed, as the residue showed only as a discoloration on the inner walls of the glass tube in which the residue had been produced. Ultrasonification with 4 mL of water in the tube showed little change to the discoloration on the inner wall of the tube. Nanodiamonds have hydrogen atoms terminating bonds at their surfaces and, since they are separated from meteorites using chemical dissolution techniques and can form colloids in mildly alkaline solutions, it was decided that a water soluble matrix such as dihydroxybenzoic acid (DHB) could be suitable for the MALDI analysis (Horneffer et al. 1999), rather than the more typical organic soluble matrices, such as sinapinic acid.

The nanodiamond suspension in water was thoroughly mixed using an ultrasonic water bath for 5 min with 10 μL of DHB solution (10 mg dissolved in 1 mL of 18MΩ water). 2 μliters of the mixture was measured onto a spot on a standard MicroTrace MALDI plate (100 stainless steel electropolished spots, a 2 mm diameter circle defined by etching). After drying and crystallization, a drop of silver trifluoroacetate dissolved in tetrahydrofuran was added as this often promotes the formation of ions in MALDI (V. Boote, personal communication). The sample was analyzed on a MicroTrace Spec2E MALDI mass spectrometer. The ions were accelerated through 25 kV and detected after their time of flight by an electron multiplier biased to −12.5 kV to enhance the detection efficiency of high mass molecules. The analyses shown here were obtained in the normal linear mode (mass resolution ~1000). Mass calibration was achieved by using the mass standard cytochrome C (12,000 Daltons) (Horneffer et al. 1999).

Two instrument characteristics determined the mass range acquired. The MicroTrace Spec2E has a selectable facility to enable the detector only after the low mass (and high abundance) ions have arrived at the detector. This was generally used in these analyses to suppress the species <2000 Daltons in the spectrum to avoid detector saturation. Furthermore, the time to digital converter of the instrument limits the maximum mass range recorded according to the time resolution chosen. For these measurements, the minimum electronic time-bin available was chosen, which limited the maximum mass recorded to 30,000 Daltons. The mass spectra illustrated in Figs. 1a and 1b were acquired including low mass ions to show the relative size of the nanodiamond peak, but most of the spectra used for analysis reported here were recorded for the mass range 2000–30,000 Daltons only.

MALDI is a technique in which it is difficult to exactly reproduce sample preparation conditions (drying and crystallization), ionization conditions, or the right conditions for high ion yield. Contamination of the sample by species such as sodium often has a drastic and detrimental effect on the ion yield; it was often necessary to fire the laser at many different places on the sample spot and see which ones yielded analyte ions. Consequently, an absence of observed analyte ions from a sample cannot automatically be taken as implying an absence of those molecules in the original sample. However, sample preparation was generally sufficiently reproducible so that control samples of the molecule cytochrome C used as the mass calibration or replicates of the meteorite samples performed at different times could be relied on to yield the same species in the mass spectra, if not always with the same efficiency or yield.

In addition, the pure DHB solution treated in the same

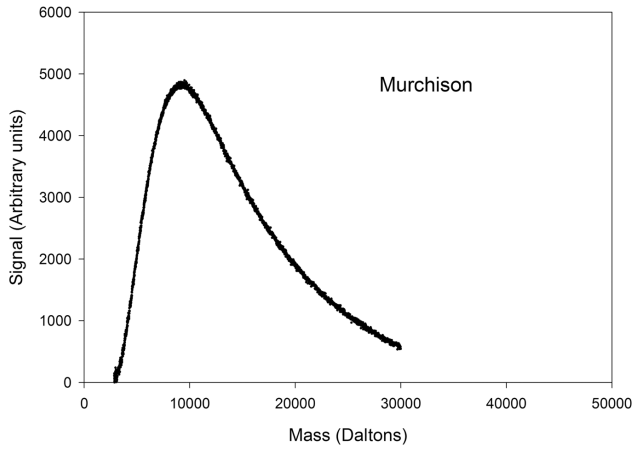

Fig. 2a. The resulting mass spectrum of Murchison nanodiamonds alone after subtraction of the background.

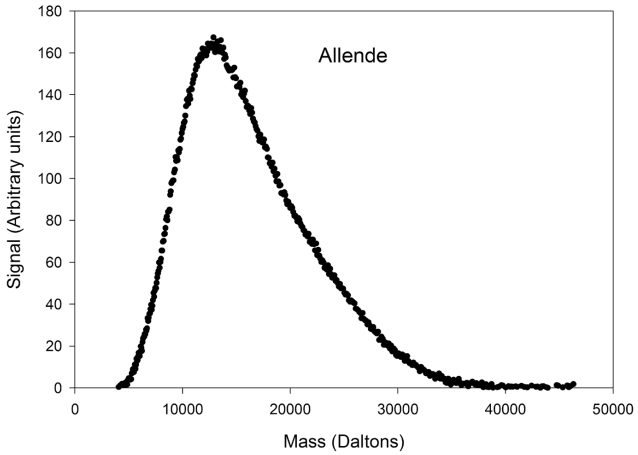

Fig. 2b. The resulting mass spectrum of Allende nanodiamonds alone after subtraction of the background. Mass bins have been averaged over 40 Daltons to reduce statistical scatter.

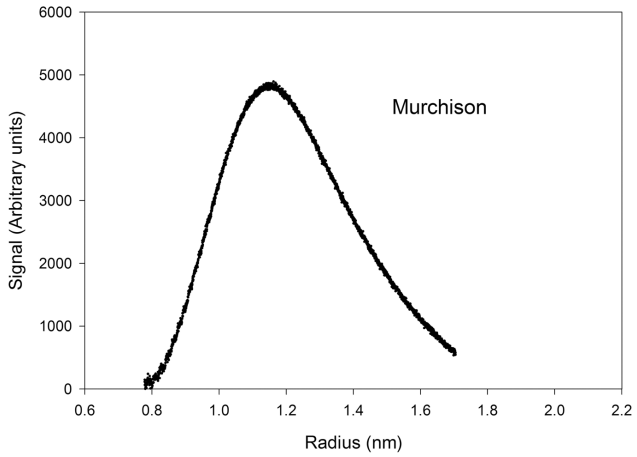

Fig. 3a. Distribution of Murchison nanodiamonds against inferred radius.

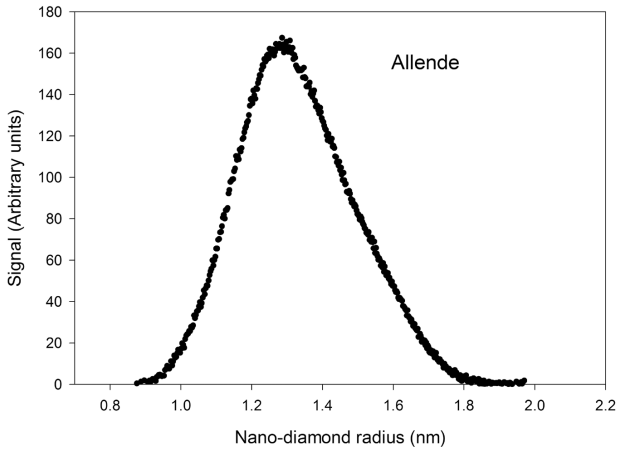

Fig. 3b. Distribution of Allende nanodiamonds against inferred radius.

way with silver trifluoroacetate in hydrotetrafuran was analyzed on numerous occasions during each analytical session to test for artifacts from the matrix that may have given the mass spectra observed. No such artifacts were observed.

RESULTS

The mass spectrum obtained from the Murchison nanodiamond separate is shown in Fig. 1a along with a mass spectrum from the DHB matrix alone in Fig. 1b. The falling tail results from a detector artifact caused by the peaks at masses <2000 Daltons being so large. The low mass ion peaks and detector background due to the DHB matrix were the same in each case so the spectrum from the matrix plus nanodiamonds and matrix alone were normalized to the same intensity in these low mass peaks and the matrix spectrum subtracted from the matrix plus nanodiamond spectrum. A wide mass peak spanning several thousand Daltons was observed centered on ~9.3 × 10^3 Daltons, corresponding to ~800 carbon atoms is shown in Fig. 2a.

The mass spectrum obtained from the Allende nanodiamonds with the background mass spectrum subtracted is shown in Fig. 2b. A large wide mass peak spanning several thousand Daltons was observed with the peak of the abundance distribution at ~1.3 × 10^4 Daltons corresponding to ~1100 carbon atoms. This peak for Allende nanodiamonds reproducibly showed a mode value that was heavier than the peak from Murchison nanodiamonds.

Lewis et al. (1987) report a bulk mean density of nanodiamonds of 2.22–2.32g cm^{-3}. If this density is assumed along with an assumption that the nanodiamonds are spherical, then the mass may be converted to equivalent radius. The resultant distributions are plotted in Figs. 3a and 3b and also as cumulative probability distributions for

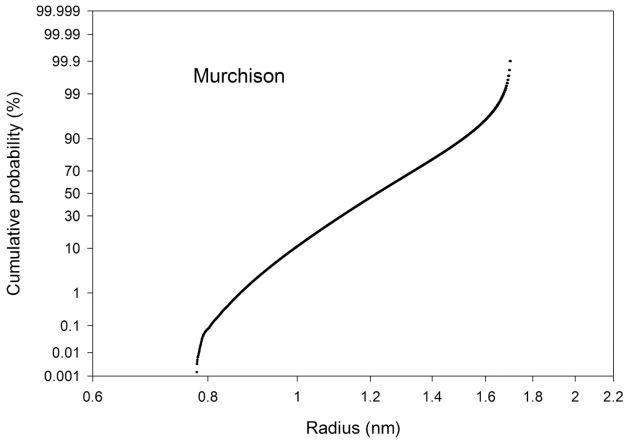

Fig. 4a. A cumulative probability plot of Murchison nanodiamonds showing deviations from a Gaussian distribution.

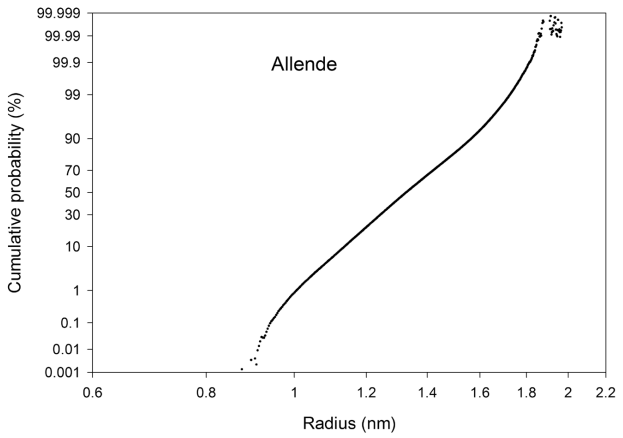

Fig. 4b. A cumulative probability plot of Allende nanodiamonds showing deviation from a Gaussian distribution.

Murchison nanodiamonds in Fig. 4a and for Allende nanodiamonds in Fig. 4b. A Gaussian distribution would plot as a straight line on these graphs.

DISCUSSION

Size distributions of nanodiamonds extracted from meteorites have been measured by point counting using transmission electron microscopy (TEM). The mean diameter for nanodiamonds found were 2.579 nm for Murchison (Daulton et al. 1996), 2.6 nm for Murchison (Lewis et al. 1989), ~2 nm for Murray by electron beam broadening (Fraundorf et al. 1989), and 2.841 nm for Allende nanodiamonds (Daulton et al. 1996).

The modal values from the mass spectra presented here peaked at ~9,300 Daltons and 13,000 Daltons. These masses are equivalent to 2.4 nm for Murchison and 2.6 nm for Allende nanodiamonds (assuming sphericity and a density of 2.22–2.32g cm^{-3}), which compare favorably with the point-counting results. The equivalent radius is clearly sensitive to the assumed density and assumption of sphericity. The 50% mean values from the cumulative probability plots (Figs. 4a and 4b) yield slightly different values of 2.4 nm for Murchison nanodiamonds and 2.7 nm for Allende nanodiamonds. The slight difference between mode and mean results from a non-symmetrical distribution that pushes the mean radius higher than the modal radius. Within possible systematic errors of 10–20%, therefore, the measurement of mean radius for nanodiamonds for both meteorites agrees between the two different methods and establishes that the ions that form the mass spectra in the MALDI-generated ion beam are primarily single nanodiamonds and not clusters.

The measured distribution of abundance with inferred radius deviates from a Gaussian distribution as evidenced by divergence from a straight line correlation on Figs. 4a and 4b. Daulton et al. (1996) also found some tendency for deviation from a log-normal distribution, although they ascribed this to systematic errors due to counting losses at both small and large nanodiamond sizes. These arose from the difficulties of counting very small nanodiamonds and undercounting large nanodiamonds due to problems with overlapping grains. The deviation from a log-normal distribution, however, is greater in the present data than found by those authors. One possible explanation is that the actual size distribution of these nanodiamonds is genuinely different from that in the residues analyzed by Daulton et al. (1996) due to minor differences in production techniques. The nanodiamond residues analyzed here were produced using the published techniques of Amari et al. (1994) and Lewis et al. (1987), but the method requires a fairly complex set of steps involving acid dissolution and recovery of nanodiamonds through colloidal separation. It is therefore possible that variations here resulted in differential recovery of different size fractions than that used by Daulton et al. (1996). It is impossible to know further whether this was a factor.

There are also possible experimental artifacts that may have induced distortions of the measured mass spectrum, as described in the following four sections.

Varying Detection Efficiency of the Ion Detector with Mass

The channel plate ion detector, like all similar detectors, has an ion detection efficiency that decreases with decreasing velocity of the impacting ion. For ions that all have the same kinetic energy, the heavier ions have lower impact velocity than lower mass ions. The channel plate detector in the MicroTrace Spec2E MALDI mass spectrometer was biased at −12.5 keV to improve detection efficiency at high masses, but nevertheless, there would be an underrepresentation of the higher mass nanodiamonds relative to lighter ions, leading to a skewed measurement of the distribution biased towards the lighter masses. However, inspection of the measured mass spectrum shows that the ions that are heavier than the modal

value are, if anything, overrepresented compared with a Gaussian distribution, so that a correction for the decreasing efficiency of the detector would only emphasize the skewness of the distribution further. Modeling the effects of non-uniformity of the detector efficiency by deliberate distortion of the measured distribution to increase the abundance of the higher mass ions (>20,000 Daltons) by up to an order of magnitude compared with the lighter mass ions (<10,000 Daltons) shows almost no effect on the deviations from a log-normal distribution shown in Figs. 4a and 4b. It is therefore concluded that the measured deviations from a Gaussian distribution do not arise from this cause.

Differential Ionization Probability with Mass

It has been assumed that the nanodiamond ions arising from the MALDI process have a uniform ionization probability with mass. This may not be true, but studies of a range of organic molecules that have been ionized by MALDI suggest that the ionization probability is uniform over the mass range of up to 10^5 Daltons (Macha and Limback 2002). To explore whether this factor could produce the deviation from a Gaussian distribution, the distribution may be varied as a function of mass, as in the Varying Detection Efficiency of the Ion Detector with Mass section. Some assumptions need to be made. Here it is assumed that if there was a varying ionization probability with mass, the ionization probability would vary with some simple, probably linear, function of mass over the mass range seen here. In that case, the conclusion from the previous section holds, so that even large variations in either detection efficiency or ionization probability produce only small shifts in the mean and modal sizes with somewhat larger effects in the tails of the distribution.

Incomplete or Incorrect Background Subtraction

The mass spectrum due to nanodiamonds appeared significantly above background noise (e.g., Figs. 1a and 1b) but nevertheless, the tail from the low mass peaks required significant correction and it is quite possible that non-optimum subtraction of this background would distort the nanodiamond spectrum, especially at the extremes of the distributions shown in Figs. 4a and 4b. This cause probably does explain the deviation from linearity of these graphs at <1% and >99%.

The Presence of Clusters of Nanodiamonds or Additional Molecules Attached to Nanodiamonds

To a good approximation, the mass spectrum matches that expected from the size distribution found by TEM point counting, which implies that most of the mass spectrum arises from single nanodiamond ions with little contamination. Molecules from the matrix or silver atoms/clusters may be attached to the nanodiamond ions. Since the chances of this happening are probably proportional to the surface area of the nanodiamonds, there is the potential for an artifact, although the added mass will be proportionally less as a fraction of the nanodiamond mass for increasing radii. This was modeled using a mass excess proportional to r^2, but even for unrealistic additions of mass at larger sizes, the cumulative probability spectrum shape was not significantly changed.

It is also possible that there is a second overlapping spectrum consisting of two or more nanodiamonds centered about ~20,000 Daltons, the shape of which would be a convolution of the nanodiamond spectrum with itself. This would tend to produce a higher count rate at the heavier masses and may therefore account for the skewed distribution of the Murchison nanodiamonds. A further possibility is that if a cluster of N nanodiamonds with a charge N+ occurs, then these would to some extent mimic the mass spectrum of single nanodiamonds, although the resultant spectra would have a wider distribution than the single nanodiamond spectrum. An argument against this possibility is that the success of MALDI relies upon the large analyte molecules being dispersed and separate in the matrix and for discrete molecules, such multiplication of mass spectra is not seen. However, in this novel case, it cannot be ruled out completely, but almost certainly makes no significant contribution to the measured mass spectrum given the close correspondence between the size distribution measured here compared with the size distributions measured by point counting.

Another effect noted from analyses of polymers is that when there is a wide distribution of masses, the available charge may limit the detectable maximum mass (Schriemer and Li 1997). This effect would tend to underrepresent the higher mass distribution contrary to the excess above a log-normal distribution found here.

CONCLUSIONS

Nanodiamond separates from the Murchison and Allende carbonaceous chondrites were mass analyzed using the MALDI technique. The mass spectra were used to infer an abundance distribution with radius for the nanodiamonds and the modal radii found were 2.4 nm for Murchison and 2.6 nm for Allende nanodiamonds. The mean values were 2.4 nm and 2.7 nm, respectively. Due to the possibility of forming a spectrum of two nanodiamond clusters that would appear at higher masses, the mode value may represent a truer value for the peak of the distribution of single nanodiamond ions, although the exact inferred radii depend on the assumed density and sphericity of the nanodiamonds. These size values compare favorably, within likely systematic errors, of values of 2.6 nm and 2.8 nm for Murchison and Allende nanodiamonds, respectively, found by Lewis et al. (1989) and Daulton et al. (1996) by TEM

point counting. The mass distribution obtained here showed some deviation from log-normal found by those authors and several potential sources of systematic error which may have caused this are discussed.

A method has been found of separating and manipulating individual nanodiamonds that opens the way to their individual analysis.

Acknowledgments–I am most grateful to Mrs. V. Boote in the School of Chemistry at the University of Manchester, UK, for help with the MALDI analysis and access to the MicroTrace Spec2E MALDI mass spectrometer, to Dr. J. Arden of the University of Oxford, UK, who produced the original Cδ separate, Mrs. C. Davies for help with chemistry preparation and clean room assistance, and to Dr. J. D. Gilmour and Professor G. Turner for helpful discussion and encouragement. I am also extremely grateful to Professors R. Lewis and A. Verchovsky and associate editor E. Zinner for very constructive reviews of this paper.

Editorial Handling—Dr. Ernst Zinner

REFERENCES

Amari S., Lewis R. S., and Anders E. 1994. Interstellar grains in meteorites: I. Isolation of SiC, graphite and diamond: Size distributions of SiC and graphite. *Geochimica et Cosmochimica Acta* 58:459–470.

Anders E. and Zinner E. 1993. Interstellar grains in primitive meteorites—Diamond, silicon-carbide, and graphite. *Meteoritics* 28:490–514.

Clayton D. D. 1989. Origin of heavy xenon in meteoritic diamonds. *The Astrophysical Journal* 340:613–619.

Clayton D. D., Meyer B. S., Sanderson C. I., Russell S. S., and Pillinger C. T. 1995. Carbon and nitrogen isotopes in type II supernova diamonds. *The Astrophysical Journal* 447:894–905.

Dai Z. R., Bradley J. P., Joswiak D. J., Brownlee D. E., Hill H. G. M., and Genge M. J. 2002. Possible in situ formation of meteoritic nanodiamonds in the early solar system. *Nature* 418: 157–159.

Daulton T. L., Eisenhour D. D., Bernatowicz T. J., Lewis R. S., and Buseck P. R. 1996. Genesis of presolar diamonds: Comparative high-resolution transmission electron microscopy study of meteoritic and terrestrial nanodiamonds. *Geochimica et Cosmochimica Acta* 60:4853–4872.

Fisenko A. V., Verchovsky A. B., Semenova L. F., and Pillinger C.T. 2004. Noble gases in the grain-size fractions of presolar diamond from the Boriskino CM2 meteorite. *Geochemistry International* 42:708–719. In Russian.

Fraundorf P., Fraundorf G., Bernatowicz T., Lewis R., and Tang M. 1989 Stardust in the TEM. *Ultramicroscopy* 27:401–412.

Horneffer V., Dreisewerd K., Lüdemann H. C., Hillenkamp F., Läge M., and Strupat K. 1999. Is the incorporation of analytes into matrix crystals a prerequisite for matrix-assisted laser desorption/ionization mass spectrometry? A study of five positional isomers of dihydroxybenzoic acid. *International Journal of Mass Spectrometry* 187:859–870.

Howard W. M., Meyer B. S., and Clayton D. D. 1992. Heavy-element abundances from a neutron burst that produces Xe-H. *Meteoritics* 27:404–412.

Huss G. R. and Lewis R. S. 1994 Noble gases in presolar diamonds I: Distinct components and their implications for diamond origins. *Meteoritics* 29:791–810.

Jurinke C., Oeth P., and van den Boom D. 2004. MALDI-TOF mass spectrometry—A versatile tool for high-performance DNA analysis. *Molecular Biotechnology* 26:147–163.

Lewis R. S., Tang M., Wacker J. F., Anders E., and Steel E. 1987. Interstellar diamonds in meteorites. *Nature* 326:160–162.

Lewis R. S., Huss G. R., and Lugmair G. 1991. Finally, Ba and Sr accompanying Xe-HL in diamonds from Allende (abstract). 22nd Lunar and Planetary Science Conference. pp. 807–808.

Lewis R. S., Anders E., and Draine B. T. 1989. Properties, detectability and origin of interstellar diamonds in meteorites. *Nature* 339:117–121.

Maas R., Loss R. D., Rosman K. J. R., de Laeter J. R., Lewis R. S., Huss G. R., and Lugmair G. W. 2001. Isotope anomalies in tellurium and palladium from Allende nanodiamonds. *Meteoritics & Planetary Science* 36:849–858.

Macha S. F. and Limbach P. A. 2002. Matrix-assisted laser desorption and ionization (MALDI) mass spectrometry of polymers. *Current Opinion in Solid State and Materials Science* 6:213–220.

Merchel S., Ott U., Herrmann S., Spettel B., Faestermann T., Knie K., Korschinek G., Rugel G., and Wallner A. 2003. Presolar nanodiamonds: Faster, cleaner, and limits on platinum-HL. *Geochimica et Cosmochimica Acta* 67:4949–4960.

Murgasova R. and Hercules D. M. 2003. MALDI of synthetic polymers—An update. *International Journal of Mass Spectrometry* 226:151–162.

Nielen M. W. F. 1999. MALDI time-of-flight mass spectrometry of synthetic polymers. *Mass Spectrometry Reviews* 18:309–344.

Ott U. 1996. Interstellar diamond xenon and time scales of supernova ejecta. *The Astrophysical Journal* 463:344–348.

Owen T., Mahaffy P. R., Niemann H. B., Atreya S., and Wong M. 2001. Protosolar nitrogen. *The Astrophysical Journal* 553:L77–L79.

Qian Y.-Z., Vogel P., and Wasserburg G. J. 1999. Neutrino fluence after r-process freezeout and abundances of Te isotopes in presolar diamonds. *The Astrophysical Journal* 513:956–960.

Reynolds J. H. and Turner G. 1964. Rare gases in the chondrite Renazzo. *Journal of Geophysical Research* 69:3263–3281.

Richter S., Ott U., and Begemann F. 1998. Tellurium in presolar diamonds as an indicator of rapid separation of supernova ejection. *Nature* 391:261–263.

Russell S. S., Arden J. W., and Pillinger C. T. 1991. Evidence for multiple sources of diamond from primitive chondrites. *Science* 254:1188–1191.

Russell S. S., Arden J. W., and Pillinger C. T. 1996. A carbon and nitrogen isotope study of diamond from primitive chondrites. *Meteoritics* 31:343–355.

Schriemer D. C. and Li L. 1997. Mass discrimination in the analysis of polydisperse polymers by MALDI time-of-flight mass spectrometry. I. Sample preparation and desorption/ionization issues. *Analytical Chemistry* 69:4169–4175.

Stump M. J., Fleming R. C., Gong W. H., Jaber A. J., Jones J. J., Surber C. W., and Wilkins C. L. 2002. Matrix-assisted laser desorption mass spectrometry. *Applied Spectroscopy Reviews* 37: 275–303.

Verchovsky A. B., Fisenko A. V., Semjonova L. F., Wright I. P., Lee M. R., and Pillinger C. T. 1998. C, N, and noble gas isotopes in grain size separates of presolar diamonds from Efremovka. *Science* 281:1165–1168.